

The influence of the symmetry of identical particles on flight times

Salvador Miret-Artés^a, Randall S. Dumont^b, Tom Rivlin^c and Eli Pollak^c

^a *Instituto de Física Fundamental, CSIC, Serrano 123, 28006 Madrid, Spain*

^b *Department of Chemistry and Chemical Biology,*

McMaster University, Hamilton, Ontario, Canada L8S 4M1 and

^c *Chemical and Biological Physics Department,*

Weizmann Institute of Science, 76100 Rehovot, Israel

Abstract

In this work, our purpose is to show how the symmetry of identical particles can influence the time evolution of free particles in the nonrelativistic and relativistic domains. For this goal, we consider a system of either two distinguishable or indistinguishable (bosons and fermions) particles. Two classes of initial conditions have been studied: different initial locations with the same momenta, and the same locations with different momenta. The flight time distribution of particles arriving at a ‘screen’ is calculated in each case. Fermions display broader distributions as compared with either distinguishable particles or bosons, leading to earlier and later arrivals for all the cases analyzed here. The symmetry of the wave function seems to speed up or slow down propagation of particles. Due to the cross terms, certain initial conditions lead to bimodality in the fermionic case. Within the nonrelativistic domain and when the short-time survival probability is analyzed, if the cross term becomes important, one finds that the decay of the overlap of fermions is faster than for distinguishable particles which in turn is faster than for bosons. These results are of interest in the short time limit since they imply that the well-known quantum Zeno effect would be stronger for bosons than for fermions. Fermions also arrive earlier than bosons when they are scattered by a delta barrier. Furthermore, the particle symmetry does not affect the mean tunneling flight time and it is given by the phase time for the distinguishable particle.

I. INTRODUCTION

It is well understood that the symmetry of indistinguishable particles has a profound influence on their dynamics. A feature which is well documented is the “bunching” of bosons [1, 2] and “anti-bunching” of fermions [3–7]. Consider two identical particles, each described for simplicity by an initial Gaussian wavepacket. When the two Gaussians of the two particles are located sufficiently far from each other in phase space, there is no overlap between them and the symmetry of particles plays no role. The fermions and bosons may be considered as two independent distinguishable particles. However, when they come close the symmetry leads to important consequences. Bosons, whose overall function is symmetric with respect to exchange may overlap with each other, hence the interference term ‘increases’ the density, causing the “bunching” phenomenon. Fermions on the other hand, due to the anti-symmetry, cannot be located at the same place and the ‘hole’ in the distribution created by the overlap term creates a distancing between the particles, which is understood as the “anti-bunching” effect.

These effects show up also in the temporal dynamics [8, 9]. Consider the scattering of two indistinguishable particles on each other and the relative distance (squared) between them as a function of time [8]. As they come closer to each other the distance is reduced and as they move again away it increases. Yet, when comparing such scattering with the exact same potential, incident energy, etc. of bosons and fermions, one finds that the distance between the fermions as they separate is larger than that of bosons – another reflection of the bunching and anti-bunching phenomenon [8, 9]. Some researchers have tried to describe the repulsion of fermions in terms of an artificial repulsive potential – the “Pauli potential”. [10–14] In statistical mechanics, this situation leads to the so-called statistical interparticle potential which is temperature-dependent since it is related to what is known as the mean thermal wavelength or thermal de Broglie wavelength. [15] One then speaks about statistical attraction and repulsion for bosons and fermions, respectively.

To the best of our knowledge the effect of symmetry on flight time distributions [16–19] has not been addressed. The central objective of this present work is to study how the symmetry affects temporal evolution, one-particle flight time distributions and, under the presence of an interaction potential, mean flight times when considering non-interacting identical particles. We will show that fermions have a broader time distribution than bosons

so that the former will be detected arriving at a suitably placed screen earlier and later, a direct result of the anti-bunching effect. Effectively, the symmetry can speed up or slow down the time evolving particles in the nonrelativistic and relativistic domains. In the second framework, we argue that one cannot speak of a superluminal effect since it can be seen as a mirror, or direct reflection, of the corresponding initial spatial distributions.

Specifically, consider first two identical particles initiated close to each other about a (mean) point in phase space, which then continue moving as free particles until they are detected on a screen some distance away. One may in principle measure the time at which a particle hits the screen and thus obtain a flight time distribution. We will show that this flight time distribution may be different for bosons and fermions as compared to distinguishable particles. The same happens when their motion is not free but they are individually scattered by a delta barrier potential.

We find that fermions have a broader time distribution than bosons, irrespective of whether they are scattered through a potential or not. Fermions will be detected arriving at the screen earlier and later than bosons, a direct result of the anti-bunching effect. A related question has to do with the survival probability of the initial wavefunction. We shall show that the bosonic survival probability of free particles decays slower than that of distinguishable particles while for fermions it decays more rapidly. These results are also of interest in the short time limit, which should imply that the well-known quantum Zeno effect [20–22] would be stronger for bosons than for fermions. However, at least for scattering through a delta potential, the particle symmetry does not affect the mean tunneling flight time and it is given by the phase time for the distinguishable particle [18, 23].

The paper is organized as follows. In Section II we consider the case of free particle propagation in the nonrelativistic and relativistic domains. In Section III the scattering of identical particles from a delta barrier potential is analyzed in detail since closed analytical expressions can be obtained. Section IV presents and discusses our results for free and tunneling dynamics. The role played by the initial width of the Gaussian wavepackets describing the identical particles in mean flight times is also analyzed. We argue that the implications of the early arrival of fermions versus bosons as, for example, photons at the screen in the relativistic case, which might seem to be superluminal, is not. It is a reflection of the anti-bunching effect on the initial density distribution. We also consider further generalizations and implications of these results to realistic systems in the last Section.

II. FREE DYNAMICS OF NONRELATIVISTIC IDENTICAL PARTICLES

A. General considerations

Our model system is two (one dimensional) non-interacting identical particles (with coordinates x_1 and x_2) and mass M which scatter from a potential $V(x_j)$. We place a screen to the right or left of the potential and measure a particle whenever it hits the screen. The questions we seek to answer are what the distribution of times at which one of the particles hits the screen is, and what the mean time it takes is, assuming that the mean time exists. The Hamiltonian for a single particle (operators are denoted with carets) is

$$\hat{H}_j = \frac{\hat{p}_j^2}{2M} + V(\hat{x}_j), j = 1, 2 \quad (2.1)$$

with \hat{p}_j and \hat{x}_j the momentum and position operators of the j -th particle respectively. The full Hamiltonian is the sum of the two

$$\hat{H} = \hat{H}_1 + \hat{H}_2. \quad (2.2)$$

Initially, the single particle wavefunction will be a coherent state localized about the mean position x_{ji} and mean momentum p_{ji} with width parameter Γ

$$\Psi_j(x_j) = \left(\frac{\Gamma}{\pi}\right)^{1/4} \exp\left[-\frac{\Gamma(x_j - x_{ji})^2}{2} + \frac{i}{\hbar}p_{ji}(x_j - x_{ji})\right], j = 1, 2. \quad (2.3)$$

To simplify, we introduce at this point the reduced coordinates of position, momenta, and time to be

$$X = \sqrt{\Gamma}x, K = \frac{p}{\hbar\sqrt{\Gamma}}, \tau = \frac{\hbar\Gamma}{M}t \quad (2.4)$$

so that the single particle wavefunction has the form

$$\Psi_j(X_j) = \left(\frac{1}{\pi}\right)^{1/4} \exp\left[-\frac{1}{2}(X_j - X_{ji})^2 + iK_{ji}(X_j - X_{ji})\right], j = 1, 2. \quad (2.5)$$

The composite wavefunction of the two particles is

$$\Psi_k(X_1, X_2) = \frac{1}{N_k} [\Psi_1(X_1)\Psi_2(X_2) + h_k\Psi_2(X_1)\Psi_1(X_2)] \quad (2.6)$$

where the coefficient h_k is

$$h_k = \begin{pmatrix} 1 \\ -1 \\ 0 \end{pmatrix} \text{ for } \begin{pmatrix} \text{bosons} \\ \text{fermions} \\ \text{distinguishable particles} \end{pmatrix} \quad (2.7)$$

and the corresponding normalization constant is

$$N_k^2 = 2 \left[1 + h_k \exp \left(-\frac{(X_{1i} - X_{2i})^2 + (K_{1i} - K_{2i})^2}{2} \right) \right], \quad k = B, F \quad (2.8)$$

where B and F denote bosons and fermions, respectively. The normalization for distinguishable particles ($k = D$) is unity. The time-evolved wavefunction is

$$\begin{aligned} N_k \Psi_k(X_1, X_2; \tau) &= \left[\exp(-i\hat{H}_1\tau) \Psi_1(X_1) \right] \left[\exp(-i\hat{H}_2\tau) \Psi_2(X_2) \right] \\ &\quad + h_k \left[\exp(-i\hat{H}_1\tau) \Psi_2(X_1) \right] \left[\exp(-i\hat{H}_2\tau) \Psi_1(X_2) \right] \\ &\equiv [\Psi_1(X_1; \tau) \Psi_2(X_2; \tau) + h_k \Psi_2(X_1; \tau) \Psi_1(X_2; \tau)]. \end{aligned} \quad (2.9)$$

We now put a ‘screen’ at the point $X = X_f$ such that the initial wave function has negligible overlap with the screen. Particle 1 may reach the screen at time τ when particle 2 is found in any location. In other words, the probability that a particle reaches the screen and that the second particle will be found at that time at some point, say, z , will be proportional to $|\Psi(X_f, X_2 = z; \tau)|^2$. We are interested in knowing the distribution of times at which a particle will hit the screen, irrespective of where the other particle is so that the probability of finding a particle hitting the screen at (the reduced) time τ is defined to be

$$P_k(X_f; \tau) = \frac{\int_{-\infty}^{\infty} dz |\Psi_k(X_f, z; \tau)|^2}{\int_0^{\infty} d\tau \int_{-\infty}^{\infty} dz |\Psi_k(X_f, z; \tau)|^2}, \quad k = B, F, D. \quad (2.10)$$

The mean time is then naturally given as

$$\langle \tau \rangle_k = \int_0^{\infty} d\tau \tau P_k(X_f; \tau), \quad k = B, F, D. \quad (2.11)$$

The distribution and the means are well defined if the time integrals converge as in potential scattering where the density decays at long times as τ^{-3} [24, 25]. For free particles, the density decays as τ^{-1} so that the best one can do is to consider the relative probability of having a particle arrive at the screen at time τ . This we denote as

$$\rho_k(X_f, \tau) = \int_{-\infty}^{\infty} dz |\Psi_k(X_f, z; \tau)|^2, \quad k = B, F, D. \quad (2.12)$$

B. Symmetry and free particles

The single free particle ($V = 0$) time evolved wavefunction is

$$\Psi_j(X, X_i, K_i, \tau) = \frac{1}{\sqrt{(1+i\tau)}} \left(\frac{1}{\pi} \right)^{1/4} \exp \left(-\frac{1}{2} \frac{[(X_j - X_{ji}) - iK_{ji}]^2}{(1+i\tau)} - \frac{K_{ji}^2}{2} \right), \quad j = 1, 2 \quad (2.13)$$

and the density is

$$|\Psi_j(X, X_{ji}, K_{ji}, \tau)|^2 = \frac{1}{\sqrt{\pi(1+\tau^2)}} \exp\left(-\frac{(X - X_{ji} - K_{ji}\tau)^2}{(1+\tau^2)}\right), j = 1, 2. \quad (2.14)$$

The free particle time-dependent density has a maximum at the (free particle) time $\tau = (X - X_{ji})/K_{ji}$. It is normalized when integrating over the position X but diverges when integrating over the time due to the long time tail which goes as $1/\tau$.

After some Gaussian integrations one finds that

$$\begin{aligned} \rho_k(X; \tau) &= \frac{1}{N_k^2} (|\Psi_1(X, X_{1i}, K_{1i}, \tau)|^2 + |\Psi_2(X, X_{2i}, K_{2i}, \tau)|^2) \\ &+ h_k \frac{2}{N_k^2} |\Psi_1(X, X_{1i}, K_{1i}, \tau)| |\Psi_2(X, X_{2i}, K_{2i}, \tau)| \\ &\exp\left(-\frac{(X_{2i} - X_{1i})^2 + (K_{2i} - K_{1i})^2}{4}\right) \cos\left(\Phi - \frac{(X_{2i} - X_{1i})(K_{2i} + K_{1i})}{2}\right), k = B, F, D \end{aligned} \quad (2.15)$$

where the phase Φ is

$$\Phi = \frac{\tau [(X - X_{1i})^2 - K_{1i}^2]}{2(1+\tau^2)} - \frac{\tau [(X - X_{2i})^2 - K_{2i}^2]}{2(1+\tau^2)} - \frac{K_{2i}(X - X_{2i})}{(1+\tau^2)} + \frac{(X - X_{1i})K_{1i}}{(1+\tau^2)}. \quad (2.16)$$

As also shown below, in the long-time limit ($\tau \rightarrow \infty$) the density scales as $\rho_k(X; \tau) \sim 1/\tau$ irrespective of whether one is considering bosons, fermions or distinguishable particles so that strictly speaking for freely evolving particles the time integral in the denominator of Eq. 2.10 diverges.

1. Bosons

If the two bosons are initially placed such that $X_{1i} = X_{2i} = X_i$ and $K_{1i} = K_{2i} = K_i$ then the phase Φ vanishes, there is no effect of interference, and the time dependent density is the same as for a distinguishable particle. Similarly, if the initial distance between the two wavepackets is sufficiently large, the interference cross term will vanish and the result will again reduce to the single particle distinguishable case. The interesting case is when the two particles are close to each other. If the initial momenta are identical, that is, $K_{1i} = K_{2i} = K_i$ ($\Delta_K = K_{2i} - K_{1i} = 0$) and the initial coordinates are written as average

and difference coordinates

$$X_i = \frac{X_{1i} + X_{2i}}{2}, \Delta_X = X_{2i} - X_{1i} \quad (2.17)$$

one finds that the density of finding a boson at the screen X at time τ

$$\rho_B(X; \tau) (\Delta_K = 0) = \frac{|\Psi(X, X_i, K_i, \tau)|^2}{\left[1 + \exp\left(-\frac{\Delta_X^2}{2}\right)\right]} \exp\left(-\frac{\Delta_X^2}{4(1 + \tau^2)}\right) \left[\cosh\left(\frac{\Delta_X(X - X_i - K_i\tau)}{(1 + \tau^2)}\right) + \exp\left(-\frac{\Delta_X^2}{4}\right) \cos\left(\frac{\tau\Delta_X[(X - X_i) - \tau K_i]}{(1 + \tau^2)}\right) \right] \quad (2.18)$$

and indeed one may check to see that

$$\int_{-\infty}^{\infty} dX \rho_B(X; \tau) = 1. \quad (2.19)$$

The long time limit is

$$\lim_{\tau \rightarrow \infty} \rho_B(X; \tau) = \frac{|\Psi_0(X, X_i, K_i, \tau)|^2}{\left[1 + \exp\left(-\frac{\Delta_X^2}{2}\right)\right]} \left[1 + \exp\left(-\frac{\Delta_X^2}{4}\right) \cos(\Delta_X K_i)\right] \quad (2.20)$$

so that as already mentioned, the free-particle time distribution of bosons decays at long time as τ^{-1} just like the single free particle.

Similarly let us consider two bosons that are initiated at the same point ($X_{1i} = X_{2i} = X_i$) but with different momenta and use the difference and mean momenta

$$K_i = \frac{K_{1i} + K_{2i}}{2}, \Delta_K = K_{2i} - K_{1i}. \quad (2.21)$$

In this case

$$\rho_B(X; \tau) (\Delta_X = 0) = \frac{2}{N^2 \sqrt{\pi} (1 + \tau^2)} \exp\left(-\frac{(X - X_i - K_i\tau)^2}{(1 + \tau^2)} - \frac{\Delta_K^2 \tau^2}{4(1 + \tau^2)}\right) \left[\cosh\left(\frac{\Delta_K \tau (X - X_i - K_i\tau)}{(1 + \tau^2)}\right) + \exp\left(-\frac{\Delta_K^2}{4}\right) \cos\left(\frac{\Delta_K [\tau K_i - (X - X_i)]}{(1 + \tau^2)}\right) \right]. \quad (2.22)$$

and this again decays at long times as τ^{-1} .

2. Fermions

Following the same algebra as in the bosonic case, one finds that the fermionic density is

$$\begin{aligned} \rho_F(X; \tau) &= \frac{1}{N_F^2} (|\Psi(X, X_{1i}, K_{1i}, \tau)|^2 + |\Psi(X, X_{2i}, K_{2i}, \tau)|^2) \\ &\quad - \frac{2}{N_F^2} |\Psi(X, X_{1i}, K_{1i}, \tau)| |\Psi(X, X_{2i}, K_{2i}, \tau)| \\ &\quad \cos\left(\Phi - \frac{(X_{2i} - X_{1i})(K_{2i} + K_{1i})}{2}\right) \exp\left(-\frac{(X_{2i} - X_{1i})^2 + (K_{2i} - K_{1i})^2}{4}\right) \end{aligned} \quad (2.23)$$

The normalization is

$$N_F^2 = 2 \left[1 - \exp\left(-\frac{\Delta_X^2 + \Delta_K^2}{2}\right) \right] \quad (2.24)$$

and it vanishes if $\Delta_X = \Delta_K = 0$ so care must be taken in this limit, since also the numerator vanishes but the ratio does not. More specifically, at time $\tau = 0$ we have with $K_{1i} = K_{2i} = K_i$ and $\Delta_X = X_{2i} - X_{1i}$

$$\begin{aligned} \lim_{\Delta_X \rightarrow 0} \Psi(X_1, X_2; 0) &= -\frac{1}{\sqrt{\pi}} (X_2 - X_1) \\ &\cdot \exp\left[iK_i (X_1 - X_{1i}) + iK_i (X_2 - X_{2i}) - \frac{1}{2} [(X_1 - X_{1i})^2 + (X_2 - X_{2i})^2] \right] \end{aligned} \quad (2.25)$$

and this vanishes if $X_1 = X_2$. Fermions cannot exist at the same point in phase space. Note however that

$$\int_{-\infty}^{\infty} dX_1 \int_{-\infty}^{\infty} dX_2 \lim_{\Delta_i \rightarrow 0} |\Psi(X_1, X_2; 0)|^2 = 1 \quad (2.26)$$

as it should be. There is no difficulty in preparing an initial wavefunction in the fermionic case even if both wavepackets are localized around the same centers both in coordinate and momentum space. The density vanishes at one point only.

Using the average and difference coordinates as above we readily find that when the two incident momenta are identical

$$\begin{aligned} \rho_F(X; \tau) (\Delta_K = 0) &= \frac{|\Psi_0(X, X_i, K_i, \tau)|^2}{2 \sinh\left(\frac{\Delta_i^2}{4}\right)} \exp\left(\frac{\tau^2 \Delta_X^2}{4(1 + \tau^2)}\right) \\ &\left[\cosh\left(\frac{\Delta_i (X - X_i - K_i \tau)}{(1 + \tau^2)}\right) - \exp\left(-\frac{\Delta_X^2}{4}\right) \cos\left(\frac{\tau \Delta_X [(X - X_i) - \tau K_i]}{(1 + \tau^2)}\right) \right]. \end{aligned} \quad (2.27)$$

It is also straightforward to see that

$$\int_{-\infty}^{\infty} dX \rho_F(X; \tau) (\Delta_K = 0) = 1. \quad (2.28)$$

When the (mean) distance between the two particles becomes small

$$\lim_{\Delta_X \rightarrow 0} \rho_F(X; \tau) = |\Psi_0(X, X_i, K_i, \tau)|^2 \left[\frac{(X - X_i - K_i \tau)^2}{(1 + \tau^2)} + \frac{1}{2} \right] \quad (2.29)$$

and at long times the fermion density is

$$\lim_{\tau \rightarrow \infty} \rho_F(X; \tau) (\Delta_K = 0) = \frac{|\Psi_0(X, X_i, K_i, \tau)|^2}{\left[1 - \exp\left(-\frac{\Delta_X^2}{2}\right) \right]} \left[1 - \exp\left(-\frac{\Delta_i^2}{4}\right) \cos(K_i \Delta_X) \right] \quad (2.30)$$

and it too decays as τ^{-1} as for bosons. The difference is only in the coefficients.

C. Survival probability and symmetry

The time-dependent overlap or survival amplitude for a single particle is

$$\begin{aligned} S_j(\tau) &= \langle \Psi(X_{ji}, K_{ji}, 0) | \Psi(X_{ji}, K_{ji}, \tau) \rangle \\ &= \sqrt{\frac{2}{(2 + i\tau)}} \exp\left(-\frac{i\tau K_{ji}^2}{(2 + i\tau)}\right). \end{aligned} \quad (2.31)$$

Analogously, the time-dependent overlap or survival amplitude for the two particle wavefunction is then

$$\Sigma(\tau) = \frac{2}{N_k^2} S_1(\tau) S_2(\tau) \left[1 + h_k \exp\left(-\frac{\Delta_X^2 + \Delta_K^2}{(2 + i\tau)}\right) \right]$$

and its square is

$$|\Sigma_k(\tau)|^2 = |S_1(\tau) S_2(\tau)|^2 O_k(\tau) \quad (2.32)$$

with

$$\begin{aligned} O_k(\tau) &= \frac{\left[1 + h_k^2 \exp\left(-\frac{4(\Delta_X^2 + \Delta_K^2)}{(4 + \tau^2)}\right) + 2h_k \exp\left(-\frac{2(\Delta_X^2 + \Delta_K^2)}{(4 + \tau^2)}\right) \cos\left(\frac{(\Delta_X^2 + \Delta_K^2)}{(4 + \tau^2)}\tau\right) \right]}{\left[1 + h_k \exp\left(-\frac{\Delta_X^2 + \Delta_K^2}{2}\right) \right]^2}, \\ k &= B, F, D. \end{aligned} \quad (2.33)$$

It is then of interest to study this overlap $O_k(\tau)$ in some limits. First, we note that when the initial distances between the wavepackets are sufficiently large, such that $\Delta_X^2 + \Delta_K^2 \gg 1$, then for times shorter than $\sim \sqrt{\Delta_X^2 + \Delta_K^2}$, this overlap function reduces to unity. This is what is expected: when the initial distance between the particles is large, they behave

as independent distinguishable particles. The interesting case is when the initial distances between the two wavepackets are small and the interference term is no longer negligible at short times. For bosons, one finds to leading order

$$\lim_{\Delta_X, \Delta_K \rightarrow 0} O_B(\tau) = 1 + \frac{(\Delta_X^2 + \Delta_K^2)\tau^2}{2(4 + \tau^2)} \geq 1 = O_D(\tau) \quad (2.34)$$

showing that in this limit, the bosonic survival probability is greater than the distinguishable particle overlap and this is so for all times. For fermions, though, one has that

$$\lim_{\Delta_X, \Delta_K \rightarrow 0} O_F(\tau) = \frac{4}{(4 + \tau^2)} \leq 1 = O_D(\tau) \quad (2.35)$$

showing that the fermionic overlap decays faster than the distinguishable particle case in this limit. In other words, when the distance in phase space between the centers of the two particles is small, which is the case when the interference term becomes most important, one finds that the decay of the overlap of fermions is faster than distinguishable particles which in turn is faster than bosons. These results are also of interest in the short time limit, where one finds that

$$\lim_{\Delta_X, \Delta_K, \tau \rightarrow 0} O_B(\tau) = 1 + \frac{(\Delta_X^2 + \Delta_K^2)\tau^2}{8} \quad (2.36)$$

$$\lim_{\Delta_X, \Delta_K, \tau \rightarrow 0} O_F(\tau) = \left(1 - \frac{\tau^2}{4}\right) \quad (2.37)$$

which indicates that the quantum Zeno effect [20–22] would be stronger for bosons than for fermions, as the fermionic survival probability decays faster also at short times.

D. Free dynamics of relativistic identical particles

To investigate the relativistic regime, we consider relativistic electrons and photons. The wavepackets describing the bosons – the photons – travel dispersion-free at the speed of light. The wavepackets describing the fermions – the electrons – are four component spinors with time evolution determined by the Dirac equation. As we consider only free particle motion of two non-interacting (except via particle statistics) electrons, spin is conserved and the wavepackets reduce to two component spinors. Relativistic wavepacket propagation is much like non-relativistic propagation except that the velocity is no longer directly proportional to wavenumber – the former asymptotes to the speed of light – and wavepacket broadening is greatly suppressed due to the dispersion relation – quadratic in the non-relativistic case

– approaching linearity. In particular, the time scale for wavepacket broadening scales with γ^2 , where $\gamma = 1/\sqrt{1 - v^2/c^2}$. (See Eq. (2.19) in [23].) For example, if $v = 0.99c$, broadening takes 50 times longer than it does for non-relativistic velocities.

The single free relativistic electron time evolved wavefunction, in the highly accurate (for cases we considered) steepest descent approximation, is

$$\Psi_j(X, X_i, K_i, \tau) = \frac{\hat{u}}{\sqrt{(1 + i(\tau/\gamma^2))}} \left(\frac{1}{\pi}\right)^{1/4} \exp\left(-\frac{1}{2} \frac{[(X_j - X_{ji}) - iK_{ji}]^2}{(1 + i(\tau/\gamma^2))} - \frac{K_{ji}^2}{2}\right), j = 1, 2, \quad (2.38)$$

where $\hat{u} = u/\|u\|$ and

$$u = \begin{pmatrix} 1 \\ \left(\frac{\hbar\Gamma^{1/2}}{mc}\right) \frac{K_{ji}}{1+\gamma} \end{pmatrix} \quad (2.39)$$

is the two component spinor for a spin up electron. This is then used in the symmetrized wavefunction for the two bosons and electrons, respectively.

IV. FLIGHT TIMES OF IDENTICAL NON-RELATIVISTIC PARTICLES SCATTERED BY A DELTA FUNCTION BARRIER

A. Preliminaries

The Hamiltonian for the delta function barrier is

$$\hat{H} = -\frac{\hbar^2}{2M} \frac{d^2}{dx^2} + \varepsilon\delta(x). \quad (4.1)$$

and the coupling coefficient $\varepsilon > 0$. The eigenfunctions of the Hamiltonian at energy

$$E = \frac{\hbar^2 k^2}{2M} \quad (4.2)$$

are

$$\psi(x) = \begin{pmatrix} \exp(ikx) + R(k) \exp(-ikx), & x < 0 \\ T(k) \exp(ikx), & x > 0 \end{pmatrix} \quad (4.3)$$

with the reflection amplitude given as

$$R(k) = \frac{-i\alpha(k)}{1 + i\alpha(k)}, \quad \alpha(k) = \frac{M\varepsilon}{\hbar^2 k}. \quad (4.4)$$

The transmission amplitude is

$$T(k) = \frac{1}{1 + i\alpha(k)} \quad (4.5)$$

and one readily sees that

$$|R(k)|^2 + |T(k)|^2 = 1. \quad (4.6)$$

The phase time delays are defined to be

$$\delta t_{T,R} = \frac{M}{\hbar k} \text{Im} \left(\frac{1}{Y} \frac{\partial Y}{\partial k} \right), \quad Y = R, T \quad (4.7)$$

so that

$$\delta t_T = \delta t_R = \frac{M}{\hbar k} \frac{\alpha(k)}{k[1 + \alpha^2(k)]} \equiv \delta t. \quad (4.8)$$

The phase time then implies that for a repulsive delta function potential ($\alpha(k) > 0$) the flight time is lengthened while for an attractive delta function potential it is shortened. In the limit that the coupling coefficient $\varepsilon \rightarrow \infty$, which is the equivalent of a hard wall potential, the transmission amplitude vanishes while the reflection amplitude goes to -1 . The reflection time delay vanishes in this case, the interference of the forward and reflected wave does not change the reflected phase time delay. For a fixed nonzero value of $\varepsilon > 0$ in the limit that the energy vanishes ($k \rightarrow 0$) the delay diverges as k^{-1} . For an attractive delta function potential, the flight time is shortened and the reduction diverges as k^{-1} . Due to the zero width of the delta function potential, the dwell time [26] in the barrier always vanishes.

It is worthwhile here also to consider the imaginary time defined as [27]

$$t_{im,R,T} = \hbar \text{Re} \left(\frac{1}{Y} \frac{\partial Y}{\partial E} \right), \quad Y = R, T \quad (4.9)$$

so that the transmitted imaginary time is positive

$$t_{im,T} = \frac{M\alpha^2(k)}{\hbar k^2 (1 + \alpha^2(k))} \quad (4.10)$$

while the reflected imaginary time is negative

$$t_{im,R} = -\frac{M}{\hbar k^2 (1 + \alpha^2(k))}. \quad (4.11)$$

As the momentum increases, the transmission probability increases while the reflection probability decreases, so that the transmitted imaginary time is positive, and the reflected is negative.

In reduced variables (with $\epsilon_i = \alpha(k)$), the phase time delay takes the simple form

$$\delta\tau(K_i) = \frac{\epsilon_i}{K_i^2(1 + \epsilon_i^2)} \quad (4.12)$$

while the imaginary time delays are

$$\tau_{im,T}(K_i) = \frac{\epsilon_i^2}{K_i^2(1 + \epsilon_i^2)} \quad (4.13)$$

and

$$\tau_{im,R}(K_i) = -\frac{1}{K_i^2(1 + \epsilon_i^2)}. \quad (4.14)$$

The transmission and reflection probabilities become

$$|T(K_i)|^2 = \frac{1}{1 + \epsilon_i^2}, |R(K_i)|^2 = \frac{\epsilon_i^2}{1 + \epsilon_i^2}. \quad (4.15)$$

1. The single particle dynamics. Momentum filtering

Initially we consider a Gaussian wavepacket as in Eq. 2.5

$$\Psi(x, 0) = \left(\frac{\Gamma}{\pi}\right)^{1/4} \exp\left[-\frac{\Gamma}{2}(x - x_i)^2 + ik_i(x - x_i)\right] \quad (4.16)$$

whose momentum representation is

$$\Psi(k, 0) = \left(\frac{1}{\pi\Gamma}\right)^{1/4} \exp\left(-\frac{(k - k_i)^2}{2\Gamma} - ikx_i\right). \quad (4.17)$$

The time dependent wavepacket in the transmitted region is

$$\Psi_T(x, t) = \int_{-\infty}^{\infty} \frac{dk}{\sqrt{2\pi}} \Psi(k, 0) T(k) \exp\left(ikx - i\frac{\hbar k^2}{2M}t\right), x \geq 0 \quad (4.18)$$

and in the reflected region is

$$\Psi_R(x, t) = \int_{-\infty}^{\infty} \frac{dk}{\sqrt{2\pi}} \exp\left(-i\frac{\hbar k^2}{2M}t\right) \Psi(k, 0) [\exp(ikx) + R(k) \exp(-ikx)], x \leq 0 \quad (4.19)$$

Using the reduced variables as in Eq. 2.4 and the reduced delta function coupling variable

$$\epsilon = \frac{M\epsilon}{\hbar^2\sqrt{\Gamma}} \quad (4.20)$$

and carrying out the momentum integrations in Eqs. 4.18 and 4.19 one finds that the transmitted time-dependent wavepacket ($X \geq 0$) is

$$\Psi_T(X, \tau) = \Psi_{fp}(X, \tau) \left[1 - \epsilon \frac{\sqrt{\pi(1+i\tau)}}{\sqrt{2}} \exp\left[-\frac{(1+i\tau)}{2}(Z_T + i\epsilon)^2\right] \operatorname{erfc}\left(-\frac{i\sqrt{(1+i\tau)}}{\sqrt{2}}(Z_T + i\epsilon)\right) \right] \quad (4.21)$$

where $\Psi_{fp}(X, \tau)$ is the free particle time-dependent wavepacket as in Eq. 2.13, erfc is the complementary error function, and

$$Z_T = \frac{[K_i + i(X - X_i)]}{(1 + i\tau)}. \quad (4.22)$$

The reflected time-dependent wavefunction ($X \leq 0$) is

$$\begin{aligned} \Psi_R(X, \tau) &= \Psi_{fp}(X, \tau) \\ &- \Psi_{fp}(-X, \tau) \epsilon \frac{\sqrt{\pi}}{\sqrt{2}} \sqrt{(1 + i\tau)} \exp\left(-\frac{(1 + i\tau)}{2} (i\epsilon + Z_R)^2\right) \text{erfc}\left(-i\sqrt{\frac{(1 + i\tau)}{2}} (i\epsilon + Z_R)\right) \end{aligned} \quad (4.23)$$

with

$$Z_R = \frac{[K_i - i(X + X_i)]}{(1 + i\tau)}. \quad (4.24)$$

In practice, if the incident (reduced) momentum is sufficiently large, which will be the case in all of our computations, and since we will be using small momentum variances, one may safely replace the complementary error function with its asymptotic expansion so that to leading order

$$\Psi_T(X, \tau) \simeq \Psi_{fp}(X, \tau) \left[\frac{Z_T}{(Z_T + i\epsilon)} \right], \quad X \geq 0 \quad (4.25)$$

and

$$\Psi_R(X, \tau) \simeq \Psi_{fp}(X, \tau) - \Psi_{fp}(-X, \tau) \frac{\epsilon}{(\epsilon - iZ_R)}, \quad X \leq 0. \quad (4.26)$$

Eqs. 4.25 and 4.26 will be the ‘workhorses’ for the numerical implementations below, but we stress that we have checked the validity of the asymptotic expansion and it is quantitative for the conditions here used. To see the long time limit we note that

$$\left| \frac{Z_T}{(Z_T + i\epsilon)} \right|^2 = \frac{[K_i^2 + (X - X_i)^2]}{[(K_i - \epsilon\tau)^2 + (X - X_i + \epsilon)^2]} \quad (4.27)$$

and this goes as τ^{-2} in the long time limit so that the transmitted single particle density decays as τ^{-3} . The calculation is a bit more involved for the reflected density but it also decays as τ^{-3} . In contrast to the free particle, due to the potential, the mean flight time (Eqs. 2.10 and 2.11) is well-defined.

We can now rewrite the density as

$$|\Psi_T(X, \tau)|^2 \simeq \frac{(1 + \tau_{fp}^2)}{\sqrt{\pi}(1 + \tau^2)} \exp\left(-\frac{K_i^2 [\tau_{fp} - \tau]^2}{(1 + \tau^2)} - \ln[(\epsilon_i\tau - 1)^2 + (\tau_{fp} + \epsilon_i)^2]\right) \quad (4.28)$$

and ask when the exponent is maximized as a function of the reduced time τ . Defining

$$G(\tau) = \frac{K_i^2 [\tau_{fp} - \tau]^2}{(1 + \tau^2)} + \ln [(\epsilon_i \tau - 1)^2 + (\tau_{fp} + \epsilon_i)^2] \quad (4.29)$$

we note that

$$\frac{dG(\tau)}{d\tau} = -2 \frac{K_i^2 [\tau_{fp} - \tau]}{(1 + \tau^2)} - 2\tau \frac{K_i^2 [\tau_{fp} - \tau]^2}{(1 + \tau^2)^2} + \frac{\epsilon_i 2 (\epsilon_i \tau - 1)}{[(\epsilon_i \tau - 1)^2 + (\tau_{fp} + \epsilon_i)^2]}. \quad (4.30)$$

Setting the derivative equal to zero

$$\frac{K_i^2 [\tau_{fp} - \tau]}{(1 + \tau^2)} + \tau \frac{K_i^2 [\tau_{fp} - \tau]^2}{(1 + \tau^2)^2} = \frac{\epsilon_i (\epsilon_i \tau - 1)}{[(\epsilon_i \tau - 1)^2 + (\tau_{fp} + \epsilon_i)^2]}. \quad (4.31)$$

and looking for a solution

$$\tau = \tau_{fp} (1 - \Delta\tau) \quad (4.32)$$

and assuming that $\Delta\tau \ll 1$ and remembering that $\tau_{fp} \gg 1$ leads to the solution

$$\Delta\tau \simeq \frac{\epsilon_i^2}{K_i^2 [1 + \epsilon_i^2]} = \tau_{im,T}(K_i) \quad (4.33)$$

and this is precisely the momentum filtering effect. Due to the increase of the transmission probability with energy, the high-energy components of the incident wavepacket are preferably transmitted so that the flight time is reduced [28].

2. Two particles dynamics

The composite initial wavefunction of the two particles is given by Eq. (2.6) and the time evolved wavefunctions by Eq. (2.9) for free particle evolution. For the δ -tunneling dynamics, the initial wave function is the same but Eq. (2.9) has to be replaced by

$$\Psi_{k,T}(X, z, \tau) = \Psi_{1,T}(X, \tau) [\Psi_{2,T}(z, \tau) + \Psi_{2,R}(z, \tau)] + h_k \Psi_{2,T}(X, \tau) [\Psi_{1,T}(z, \tau) + \Psi_{1,R}(z, \tau)] \quad (4.34)$$

for the total transmitted wavefunction and

$$\Psi_{k,R}(X, z, \tau) = \Psi_{1,R}(X, \tau) [\Psi_{2,T}(z, \tau) + \Psi_{2,R}(z, \tau)] + h_k \Psi_{2,R}(X, \tau) [\Psi_{1,T}(z, \tau) + \Psi_{1,R}(z, \tau)] \quad (4.35)$$

for the total reflected wavefunction, $\Psi_{1,T}$, $\Psi_{2,T}$, $\Psi_{1,R}$ and $\Psi_{2,R}$ being the transmitted and reflected wave functions for each particle when considered to be independent. The one-particle mean flight time is given by

$$\langle \tau_k \rangle_{T,R} = \int_0^\infty d\tau \tau P_{k;T,R}(X_f, \tau), \quad (4.36)$$

where the probability distribution is

$$P_{k;T,R}(X_f, \tau) = \frac{\int_{-\infty}^{\infty} dz |\Psi_{k;T,R}(X_f, z; \tau)|^2}{\int_0^{\infty} d\tau \int_{-\infty}^{\infty} dz |\Psi_{k;T,R}(X_f, z, \tau)|^2} \quad (4.37)$$

with $k = D, B, F$. The screen is located at $X = \pm X_f$ depending on whether we are considering the transmitted (plus sign) or reflected (minus sign) total wave function. As mentioned above, these distributions and mean times are well defined under the presence of a potential since the density decays at long times as τ^{-3} .

V. NUMERICAL RESULTS

A. Free particle non-relativistic flight times

To analyze the role played by the symmetry of the total wave function in systems of identical particles when considering free dynamics and tunneling from a delta barrier, we have identified two types of initial conditions (in reduced coordinates): (I) different locations with the same momenta, $X_{1i} = -301$, $X_{2i} = -299$ with $K_{1i} = K_{2i} = 10$ and (II) the same locations with different momenta, $X_{1i} = X_{2i} = -300$ with $K_{1i} = 10.1$ and $K_{2i} = 9.9$. When the differences in initial positions and momenta differ more, the cross terms in the density of the two-particle system become smaller, and one rapidly reaches the distinguishable particle limit. Unless otherwise stated, we will assume $\Gamma = 0.01$ for the initial width of the Gaussian functions and $\epsilon = 1$, for the strength of the coupling to the delta barrier. In all cases, the position of the screen is at $X_f = \pm 450$ and the delta barrier is located at the origin.

In Figure 1, we plot the initial spatial distributions (left panels) and (see Eq. 2.12) the one-particle flight time distributions (right panels) for the two sets of initial conditions. The top two panels are for case (I) (initial spatial difference) the bottom two are for case (II) (initial momentum difference). The solid red curve is used for distinguishable particles, the long-dashed blue curve for bosons and the dot-dashed brown curve for fermions. The one-particle flight time distribution is broader for fermions displaying early and late arrivals. Bosons tend to arrive later than distinguishable particles, showing the narrowest time distribution. Furthermore, the flight time distributions of distinguishable particles and bosons tend to have a similar shape, losing the two lobes of the initial density, whereas the fermions display a double-peaked time distribution, reflecting their initial density. In the bottom-right

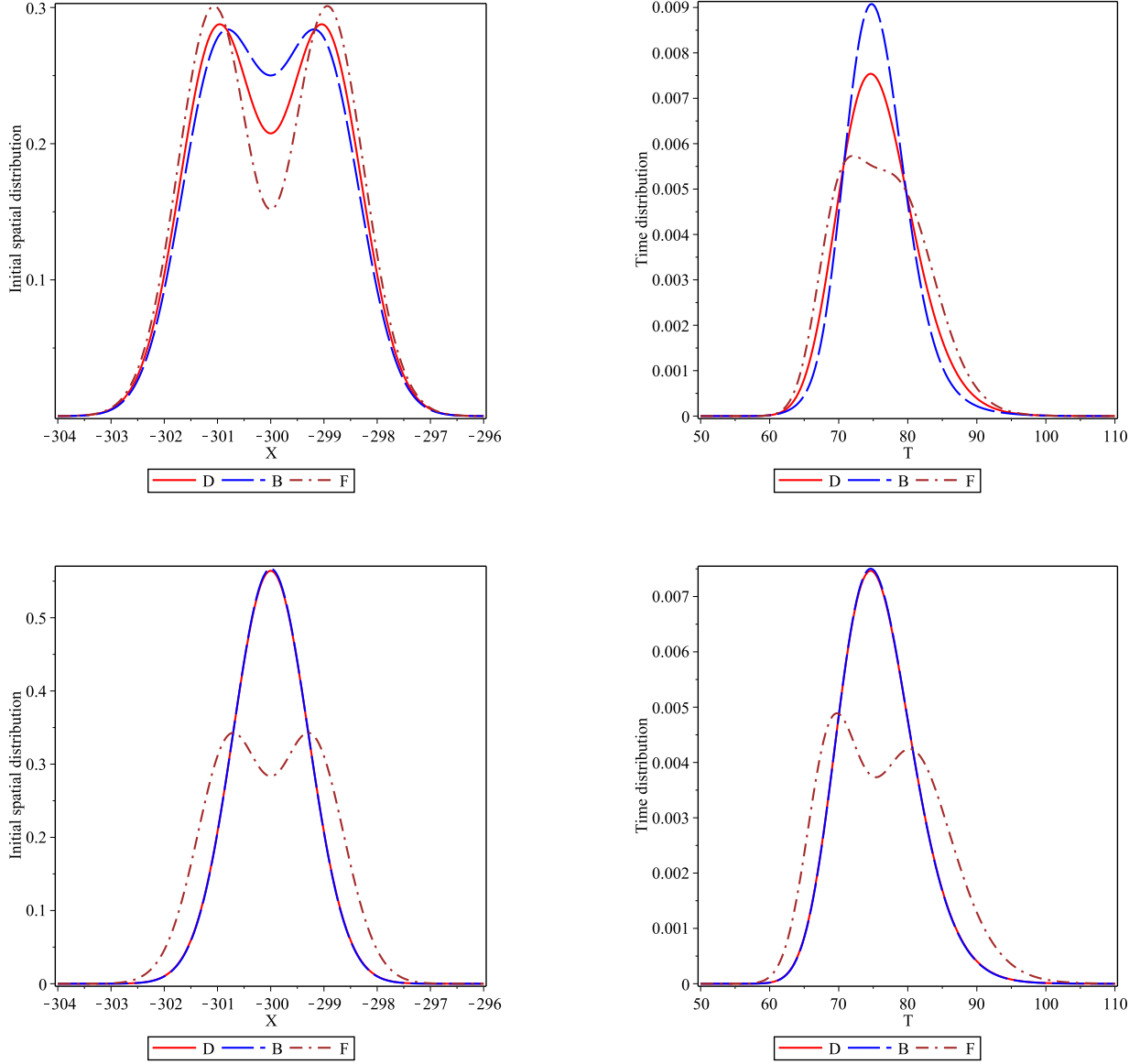


FIG. 1: Non-relativistic free particle dynamics. The left panels show the initial spatial distribution, the right panels the relative one particle flight time distributions as defined in Eq. 2.21 hitting the screen located at $X_f = 450$. The other parameters used are $\Gamma = 0.01$ for the initial width of the coherent states; for case (I) (initial spatial difference) $X_{1i} = -301$, $X_{2i} = -299$, $K_{1i} = K_{2i} = 10$, left and right top panels; and for case (II) (initial momentum difference) $X_{1i} = X_{2i} = -300$, $K_{1i} = 10.1$, $K_{2i} = 9.9$, left and right bottom panels.

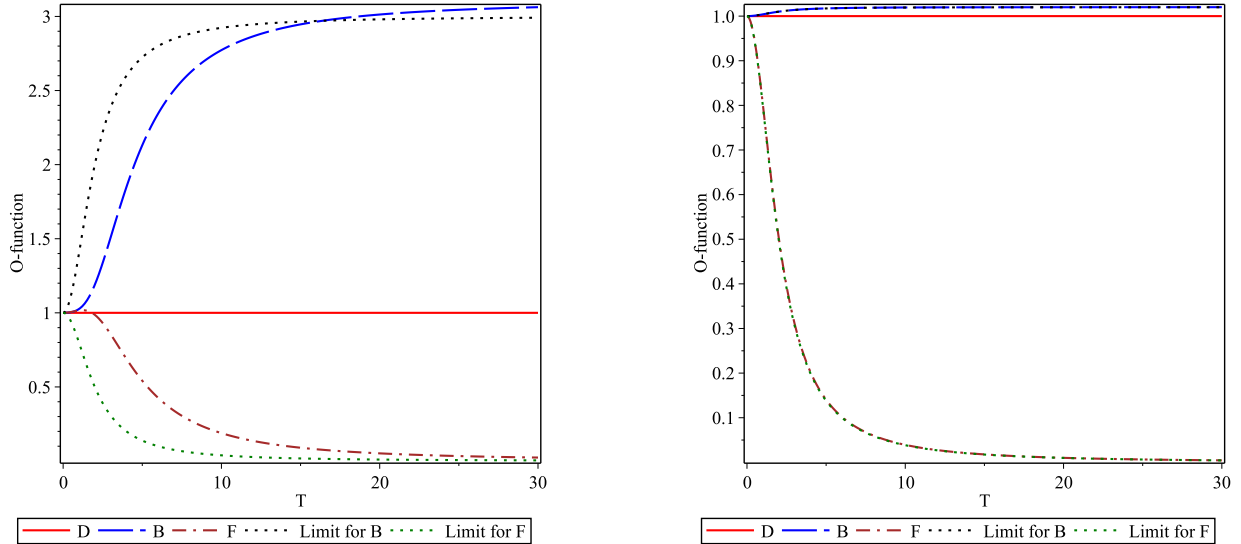


FIG. 2: Overlap decay (O-function) defined in Eq. 2.33 for non-relativistic free particles. The left and right panels are for initial spatial (case I) and momentum (case II) differences, respectively. The initial width of the Gaussians here is taken to be $\Gamma = 0.01$.

panel, bosons and distinguishable particles behave essentially identically whereas fermions display a bimodal time distribution. Fermions not only arrive at the screen earlier and later, there is a distinctive time asymmetry in the flight time distribution. We attribute these different behaviors to the bunching and anti-bunching properties of bosons and fermions, respectively. Specifically, the early arrival of fermions at the screen is related to the ‘front’ of the initial fermionic density distribution, which, due to the anti-bunching effect, is closer to the origin than in the case of bosons and distinguishable particles. The same is true for the portion of the fermionic flight time distribution which arrives later at the barrier. It is due to the back of the initial fermionic density which is further from the origin, when compared to bosons or distinguishable particles.

In a previous work where we studied the MacColl-Hartman effect we have argued against the ‘front’ of the wavepacket being used to explain away supposedly superluminal propagation for *tunneling* particles [18, 23], noting that the superluminality cannot be used for the purpose of early signaling. When considering the MacColl-Hartman effect, one is comparing final time distributions of tunneled particles with free particles, but the two have the same initial density distribution. In the case considered here, the initial wavepacket of the

fermions is broadened when compared to that of the bosons. It is this broadening which leads to early and late arrival times of fermions as compared to bosons, meaning that one does not have to consider here the possibility of superluminality.

Another interesting aspect considered here is the analysis of the survival amplitude, using Eq. (2.33) and the limits at small initial spatial Δ_X and momentum Δ_K difference and the associated time dependence, as in Eqs. (2.36) and (2.37). In Figure 2 we plot the overlapping functions (O-function, see Eq. 2.33) for initial conditions (I) (initial spatial difference) in the left panel and for case (II) (initial momentum difference) in the right panel. As in Fig. 1, the red line indicates the behavior for distinguishable particles, the long-dashed blue curve is used for bosons and the dot-dashed brown curve for fermions. Dotted black and green curves correspond to the limits of small values of Δ_X , Δ_K and time. The time dependence of the corresponding overlapping functions is quite different for bosons and fermions. The bosons stay together for a long time whereas the fermionic overlap decays rapidly.

B. Free particle relativistic flight time distributions

Figure 3 shows the time-dependent density at the screen (at $X = 0$) for two photons and two electrons traveling near the speed of light. In the left panel, the two Gaussians are centered at $X_{1i} = -3.5$ and $X_{2i} = -3$ and at a wavenumber consistent with velocity, $v = 0.99c$. In the right panel, the two Gaussians are centered at $X_{1i} = X_{2i} = -3$ and at wavenumbers consistent with $v = 0.984c$ and $0.996c$. In both cases, an electron is more likely to arrive at the screen before a photon. However, this is simply because the initial density for the electrons is broader than that of the photons. To show this, the density that would be seen if the electrons traveled dispersion-free at the speed of light is also shown (dotted lines). The observed electron density clearly travels with a speed less than c . The early and late arrivals of the fermions is just a reflection of their initial density, which, as may be seen from the left panels of Fig. 1, is broader than the initial distribution for bosons, due to the anti-bunching effect of fermions. The early arrival times are a reflection of the initial width of the packet – this is the same for both the relativistic and the non-relativistic regimes.

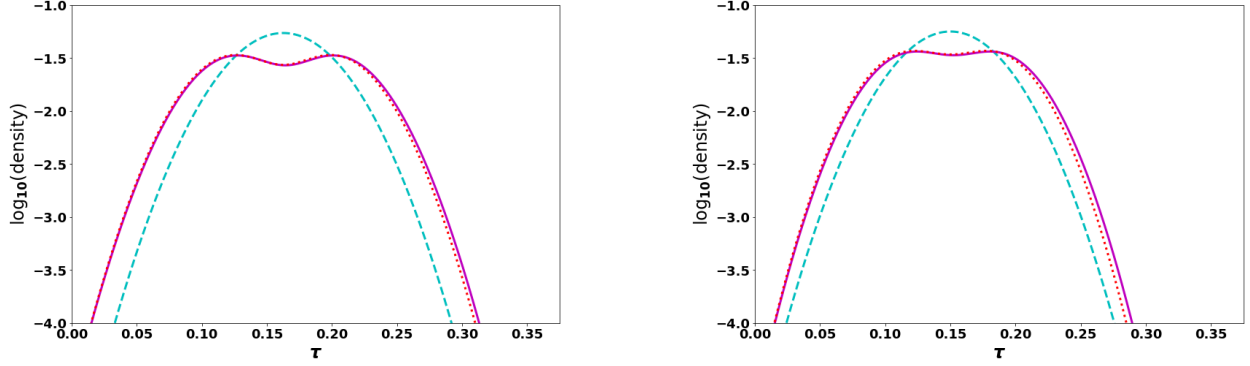


FIG. 3: Time-dependent densities for two photons (dashed lines) and two relativistic electrons (solid lines). The left and right panels are for initial spatial (case I) and momentum (case II) differences, respectively. The initial width of the Gaussians here is taken to be $\Gamma = 0.0025$. Also shown (dotted lines) are the densities that would be seen if the electrons traveled dispersion-free at the speed of light.

TABLE I: Initial conditions and transmitted (T) and reflected (R) mean flight times (in reduced coordinates) for bosons, $\langle \tau_{1,B} \rangle_{T,R}$, and fermions, $\langle \tau_{1,F} \rangle_{T,R}$, with $\Gamma = 0.01$ and $\varepsilon = 1$.

X_{1i}	X_{2i}	X_f	K_{1i}, K_{2i}	$\langle \tau_{1,B} \rangle_T$	$\langle \tau_{1,B} \rangle_R$	$\langle \tau_{1,F} \rangle_T$	$\langle \tau_{1,F} \rangle_R$
-301	-299	± 450	10, 10	75.2908	75.8847	75.4992	76.5237
-300	-300	± 450	10.1, 9.9	75.3749	76.1740	76.7417	77.3525

C. Identical particle, non-relativistic flight times for scattering on a delta potential barrier

In this case, as noted above, the mean flight times (Eq. 2.10) are well defined, and they provide a clear measure of the effect of particle symmetry on the flight time. In Table I, we provide the transmitted and reflected mean flight times (in reduced coordinates) for bosons $\langle \tau_{1,B} \rangle_{T,R}$ and fermions $\langle \tau_{1,F} \rangle_{T,R}$ with $\Gamma = 0.01$ and $\varepsilon = 1$ for the two cases of initial spatial (I) and momentum (II) differences. Transmitted mean times are always shorter than reflected mean times due to the momentum filtering effect and those of fermions are always greater than for bosons due to their anti-bunching and bunching properties.

The corresponding flight time probability distributions (eq. 2.11) are shown in Fig. 4. The top and bottom panels correspond to initial spatial (case I) and initial momentum (case II) differences, the left and right panels correspond to the transmitted and reflected flight time distributions, respectively. The trends are similar to those found in the free particle dynamics scenario. The effect of symmetry on flight times seems to be robust and is not changed much in the presence of an interaction barrier. Time distributions are broadest for fermions and narrowest for bosons, with distinguishable particles in between. The asymmetry of the bimodal reflected distributions for fermions becomes less important when comparing with the transmitted ones.

Finally, it is also of interest to analyze the role played by the initial width (Γ) of the Gaussian wavepackets in the mean tunneling flight times which are well defined, especially when Γ approaches zero such that the spatial extent of the two Gaussians is large, which creates large initial overlaps. This analysis is carried out by means of a fitting procedure to a linear function ($b\Gamma + c$) obtained from the numerics for eight values of the initial width, $\Gamma = 10^{-2}, 0.25 \cdot 10^{-2}, 9.0 \cdot 10^{-4}, 4.0 \cdot 10^{-4}, 10^{-4}, 0.25 \cdot 10^{-4}, 9.0 \cdot 10^{-6}, 4.0 \cdot 10^{-6}$. In Figure 5, the transmitted (left panel) and reflected (right panel) mean flight times versus Γ for distinguishable particles, bosons and fermions are plotted. The legend is the same one used along this work for each particle. In every case, the quality of the fitting is very good. All particles tend to a value of $c = 75.005$, which is the phase time under conditions (I). Thus, the symmetry seems to play no role in the mean tunneling flight times since the phase time for a single particle is recovered in the limit $\Gamma \rightarrow 0$.

VI. DISCUSSION

In this work, we have analyzed the influence of the symmetry of the wavefunction for a system consisting of two non-interacting identical particles. The well-known bunching and anti-bunching properties exhibited by bosons and fermions respectively have been translated into the spreading of the initial spatial densities and flight time distributions under the presence or not of an interaction potential such as a delta barrier, leading to early arrivals for fermions. Interestingly, the symmetry of the wave function seems to be robust for flight time distributions, but it does not affect the mean tunneling flight times. Analyzing the short-time dynamics through the survival probability, fermions tend to decay faster than

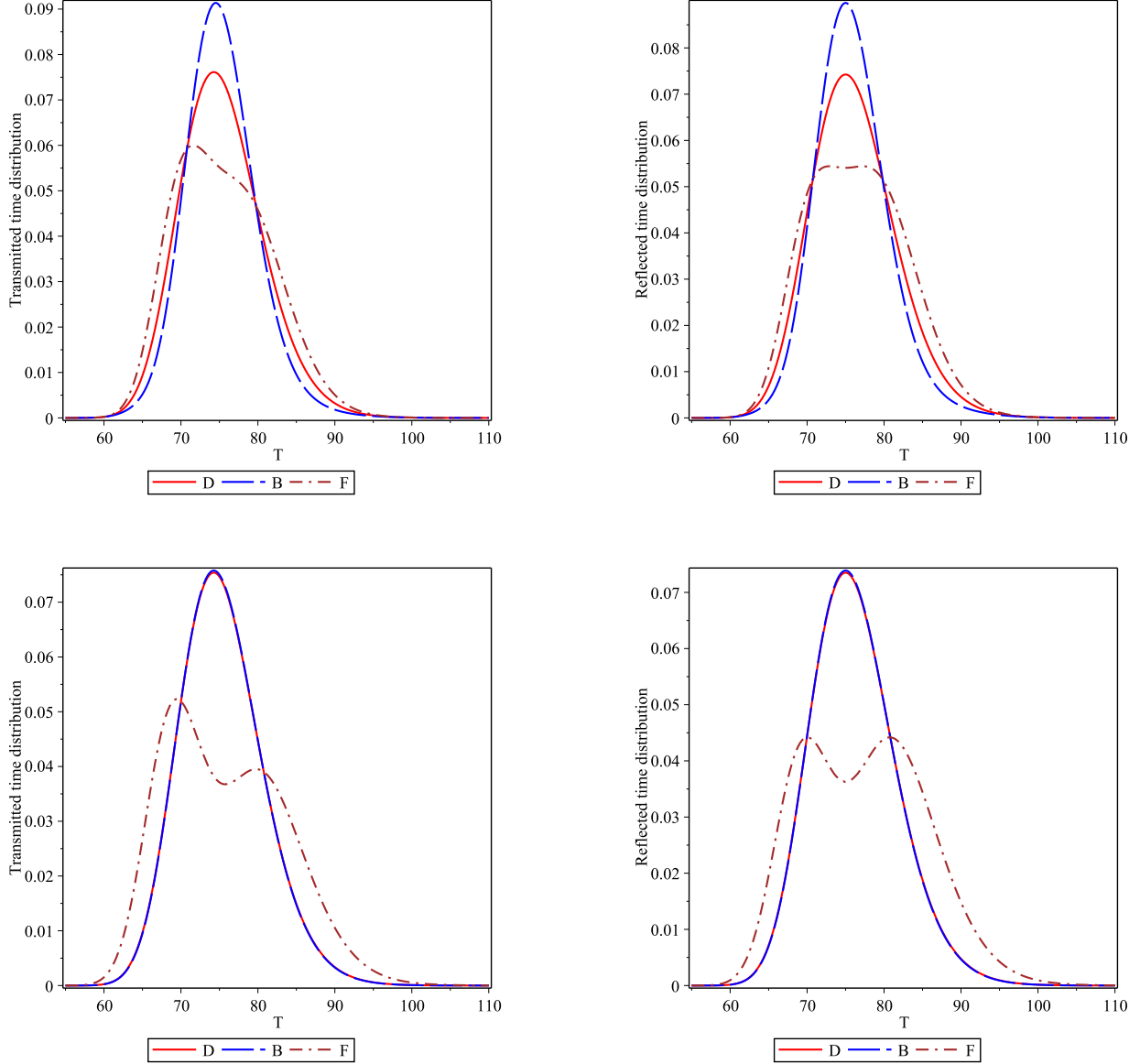


FIG. 4: Tunneling δ -barrier dynamics with $\Gamma = 0.01$. One-particle transmitted and reflected mean flight time distributions for conditions (I) are shown in the left and right top panels and for conditions (II) in the left and right bottom panels.

bosons, which has profound implications for the well-known Zeno effect.

In our model, we have considered non-interacting identical particles. This is clearly an oversimplification of the real problem since, for example, electrons interact with each other through the long-range Coulomb repulsion. As far as we know, very few studies have addressed the issue of the effect of symmetry on flight times and the Zeno effect even

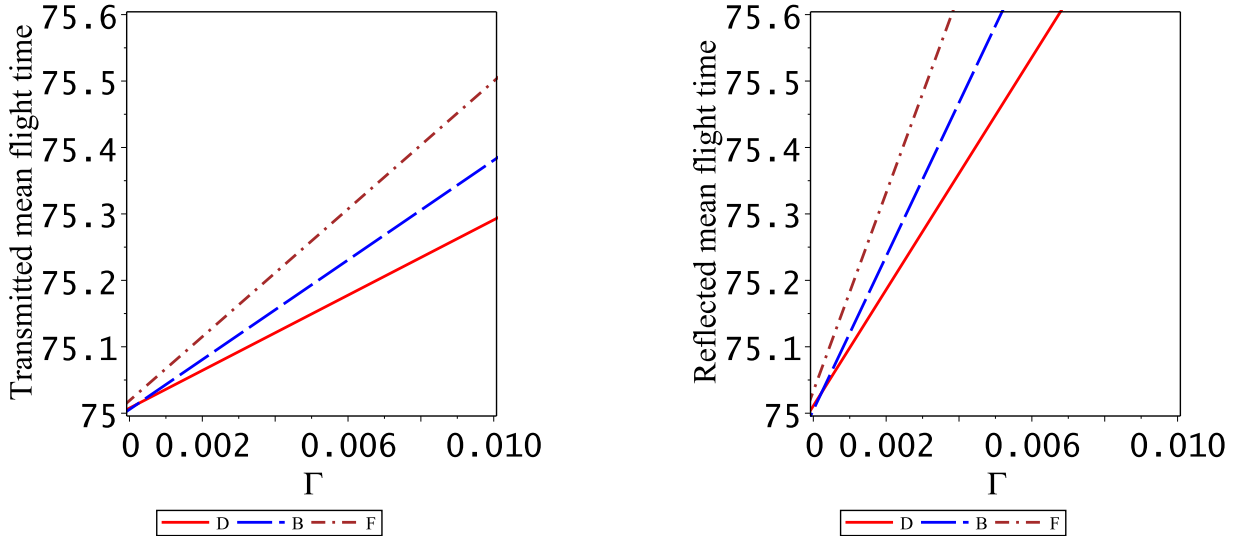


FIG. 5: One-particle transmitted (left panel) and reflected (right panel) mean flight times versus Γ for distinguishable particles, bosons and fermions under conditions (I). The legend is the same one used along this work for each particle.

though it should be readily accessible. For example, the triplet states of two electrons will give a fermionic spatial wavefunction while the singlet state a bosonic one. In a scattering experiment similar to the one discussed in Refs. [8, 9], the two particles in the center of mass frame will approach each other such that the distances between the two particles becomes small and the symmetry will affect the time of flight distribution of the two particles. Due to the anti-bunching property of fermions, one should expect broader temporal distributions of the scattered particles.

Lozovik *et al* [29] considered tunneling of two interacting particles in a double-well potential. They used quantum molecular dynamics within the Wigner representation and found that exchange effects are very important and affect the tunneling. However, this work does not mention flight time distributions. It is thus possible, at least in principle, to study the effect of particle symmetry on flight time distributions of identical electrons, without neglecting the repulsive potential of interaction between them, though the actual numerical implementation, especially in the relativistic regime is much more challenging.

Finally, we note that the study of symmetry on flight time distributions presented in this paper may be generalized to anyons, by introducing a phase in the initial distribution.

Acknowledgements TR and EP acknowledge support from the Israel Science Foundation, SMA acknowledges support from the Ministerio de Ciencia, Innovación y Universidades (Spain) under the Project FIS2017-83473-C2-1-P and Fundación Humanismo y Ciencia.

- [1] R. Hanbury Brown and R. Q. Twiss, *Nature (London)* **177**, 27 (1956).
- [2] T. Jelte, J. M. McNamara, W. Hogervorst, W. Vassen, V. Krachmalnicoff, M. Schellekens, A. Perrin, H. Chang, D. Boiron, A. Aspect and C. I. Westbrook, *Nature* **445**, 402 (2007).
- [3] M. Henny et al, *Science* **284**, 296 (1999).
- [4] W.D. Oliver, J. Kim, R.C. Liu, and Y. Yamamoto, *Science* **284**, 299 (1999).
- [5] H. Kiesel, A. Renz, and F. Hasselbach, *Nature* **418**, 392 (2002).
- [6] M. Iannuzzi, A. Orecchini, F. Sacchetti, P. Facchi and S. Pascazio, *Phys. Rev. Lett.* **96**, 080402 (2006).
- [7] T. Rom, Th. Best, D. van Oosten, U. Schneider, S. Foelling, B. Paredes and I. Bloch, *Nature* **444**, 733 (2006).
- [8] F. Grossmann, M. Buchholz, E. Pollak, and M. Nest, *Phys. Rev. A* **89**, 032104 (2014).
- [9] M. Buchholz and F. Grossmann, *J. Phys.: Conf. Ser.* **1071**, 012004 (2018).
- [10] L. Wilets, E.M. Henley, M. Kraft, and A. MacKellar, *Nucl. Phys. A* **282**, 341 (1977).
- [11] C. Dorso, S. Duarte, and J. Randrup, *Phys. Lett. B* **188**, 287 (1987).
- [12] D. H. Boal and J. N. Glosli, *Phys. Rev. C* **38**, 1870 (1988).
- [13] V. Latora, M. Belkacem, and A. Bonasera, *Phys. Rev. Lett.* **73**, 1765 (1994).
- [14] B. Gu, V. Rassolov and S. Garashchuk, *Theor. Chem. Acc.* **135**, 267 (2016).
- [15] R. K. Pathria and P. D. Beale, *Statistical Mechanics*, Elsevier, Third edition, 2011.
- [16] J. Petersen and E. Pollak, *J. Phys. Chem. Lett.* **8**, 4017 (2017).
- [17] J. Petersen and E. Pollak, *J. Phys. Chem. A* **122**, 3563 (2018).
- [18] T. Rivlin, E. Pollak and R.S. Dumont, *Phys. Rev. A* **103**, 012225 (2021).
- [19] R. Ianculescu and E. Pollak, *Phys. Rev. A* **103**, 042215 (2021).
- [20] B. Misra and E. C. G. Sudarshan, *J. Math. Phys.* **18**, 756 (1977).
- [21] P. Facchi and S. Pascazio, *J. Phys. A: Math. Theor.* **41**, 493001 (2008).
- [22] A. S. Sanz, C. Sanz-Sanz, T. González-Lezana, O. Roncero and S. Miret-Artés, *Ann. Phys.*

- 327**, 1277 (2012).
- [23] R.S. Dumont, T. Rivlin and E. Pollak, *New J. Phys.* **22**, 093060 (2020).
- [24] G. Muga, *Lect. Notes Phys.* **734**, 31 (2008).
- [25] E. Pollak and S. Miret-Artés, *New J. Phys.* **20**, 073016 (2018).
- [26] J. G. Muga, R. Sala Mayato and I. L. Egusquiza, Eds. *Time in Quantum Mechanics 1*, *Lect. Notes Phys.* **734**, 2008.
- [27] E. Pollak and W. H. Miller, *Phys. Rev. Lett.* **53**, 115 (1984).
- [28] Yu. E. Lozovik and A. V. Filinov, *JETP* **88**, 1026 (1999)
- [29] Yu E. Lozovik, A. V. Filinov and A. S. Arkhipov, *Phys. Rev. E* **67**, 026707 (2003)